

MULTISCALE DAMAGE ANALYSIS OF A PLAIN CARBON WEAVE INCORPORATING MATERIAL VARIABILITY

L.F. Varandas¹, A.R. Melro², G. Catalanotti¹ and B.G. Falzon¹

¹Advanced Composites Research Group (ACRG), School of Mechanical and Aerospace Engineering,
Queen's University Belfast, Belfast BT9 5AH, UK

²Bristol Composites Institute (ACCIS), University of Bristol, BS8 1TR, UK

Email: L.Varandas@qub.ac.uk, Web Page: <https://www.qub.ac.uk/sites/acrg/>

Email: antonio.melro@bristol.ac.uk, Web Page: <https://www.bristol.ac.uk/composites/>

Email: G.Catalanotti@qub.ac.uk, Web Page: <https://www.qub.ac.uk/sites/acrg/>

Email: B.Falzon@qub.ac.uk, Web Page: <https://www.qub.ac.uk/sites/acrg/>

Keywords: Textile composites, Mechanical properties, Computational mechanics, Finite Element Analysis (FEA), Multiscale modelling

Abstract

The mechanical behaviour and progressive damage of a plain woven carbon-epoxy fabric at different length scales is modelled, taking into account the weave's geometric, and consequently, material variability. Micromechanical simulations are performed with different fibre volume fractions using a fibre distribution algorithm in order to obtain the mechanical properties of the tows along their length. A Representative Unit Cell (RUC) is generated and a set of in-plane Periodic Boundary Conditions (PBCs) implemented in order to run non-homogenised mesomechanical analyses. The influence of material variability is captured through volumetric homogenisation to study damage evolution and corresponding stiffness degradation in a plain weave fibre architecture under different loading conditions.

1. Introduction

Two-dimensional plain weave is one of the most widely used textiles in composites production, thus it is critical to be able to evaluate and predict damage initiation and propagation in this type of material. It is still not completely clear how damage evolves in this type of textile composite, since different internal geometries of the material may lead to different stress concentration areas, crack propagation patterns and final failure scenarios. The changes in geometrical parameters, such as the height and width of a tow along its length [1] cause intra-tow fibre volume fraction variability which may lead to different homogenised mechanical properties. Neglecting this variability may lead to a reduction in accuracy of numerical predictions.

The present multiscale model represents a link between the microscale, which is described by a Representative Volume Element (RVE), discretizing the constituents and their interface, and the non-homogenised mesoscale, described by a Representative Unit Cell (RUC), encompassing the epoxy matrix (same as the one used in the micromechanical model) and homogenised tows. Micromechanics has emerged as an accurate and reliable tool to study the mechanical response of laminated composites [2]–[6]. So, using appropriate constitutive material models, it is possible to evaluate the effect of the intra-tow fibre volume fraction variability on the mechanical response of a woven carbon-epoxy fabric.

2. Multiscale model

2.1. Material constitutive models

The epoxy matrix is modelled using the elastic-plastic constitutive damage model proposed by Melro et al. [7], implemented as a VUMAT user subroutine of the Finite Element (FE) commercial software Abaqus[®] [8]. The initial elastic behaviour is defined by a linear relation between the stress and elastic strain tensor. A paraboloidal yield criterion, originally proposed by Tschoegl [9], defined as a function of the stress tensor and of the compressive and tensile yield strengths, is used together with a non-associative flow rule. A thermodynamically consistent isotropic damage model, defined by a single damage variable is used, where damage onset is defined by a damage activation function similar to the paraboloidal yield criterion, but using the final compressive and tensile strengths of the epoxy matrix instead of yield strengths and the concept of effective stress tensor, i.e. the stress tensor calculated using the undamaged stiffness tensor. To avoid mesh size dependency, Bažant and Oh's crack band model [10], which uses the individual characteristic element length and the mode I fracture toughness of the epoxy to regularise the computed dissipated energy, is implemented along with the definition of a damage evolution law [7].

The fibres are considered to be linear elastic up to failure and to have a transversely isotropic behaviour. The damage model is activated solely by the longitudinal stress component, thus, only one damage variable is used.

The fibre-matrix interface is modelled using cohesive elements of the FE commercial software Abaqus[®] [8]. Before damage initiation, a linear traction separation behaviour is assumed. The initiation of the softening process is predicted using a stress-based quadratic failure criterion. Damage evolution is based on the energy dissipated as a result of the damage process, adopting an exponential softening response under mode I, mode II or mixed-mode, according to BK law [11].

The tows presented at the non-homogenised mesoscale framework are modelled using a transverse isotropic intralaminar damage model developed by the Advanced Composites Research Group (ACRG) at Queen's University Belfast [12]–[15]. Faggiani and Falzon [12] combined Continuous Damage Mechanics (CDM) with the appropriate damage initiation criteria to produce a response model that is suitable for simulating impact damage on unidirectional composite panels. For simulating the materials' crush response, i.e. a complex loading state with several damage interactions, additional features and/or modifications to the initial model were made to account for load reversal, stiffness degradation, capturing the in-situ effect [16], element objectivity [14], element deletion criteria [13] and non-linear shear behaviour [15].

2.2. Details of the FE models: geometry, boundary conditions and material properties

Both models are subjected to Periodic Boundary Conditions (PBCs). This type of boundary condition is used due to the fact that multiple authors have concluded that the overall properties of the lower scale models are better estimated using PBCs [17]–[19]. The micromechanical model, i.e. the RVE, is subjected to three-dimensional PBCs, however, the model at the non-homogenised mesoscale is subjected to bi-dimensional (in-plane) PBCs, which are achieved by eliminating equations that establish a kinematic link between opposite faces along the out-of-plane direction [20].

The RVEs are generated using a modification of an algorithm developed by Catalanotti [21], which is able to create random distributions of uniform spherical or circular particles for any given fibre volume fraction. The mechanical properties of the constituents and of the fibre-matrix interface are represented in Tables 1 and 2, respectively.

Table 1. Properties of constituents.

Mechanical property	AS4 Fibres [22]	Epoxy matrix [4]
E_{11} [MPa]	225000	3760
E_{22} [MPa]	15000	3760
G_{12} [MPa]	15000	1352
G_{23} [MPa]	7000	1352
ν_{12}	0.2	0.39
X_T [MPa]	3350	93
X_C [MPa]	2500	180
G_I^c [N/mm]	4×10^{-3}	0.09

Table 2. Properties of fibre-matrix interface.

Mechanical property	Fibre-matrix interface [2], [4]
K [N/mm ³]	10^8
τ_1^0 [MPa]	75
τ_2^0 [MPa]	75
τ_3^0 [MPa]	50
G_I^c [N/mm]	0.002
G_{II}^c [N/mm]	0.006
G_{III}^c [N/mm]	0.006
η	1.45

At the non-homogenised mesoscale, two different RUCs are generated: i) having a constant cross-sectional area and consequently constant mechanical properties along the tow, and ii) a non-constant cross-sectional area (Figure 1), causing intra-tow fibre volume fraction variability [1], [23], leading to different mechanical properties along the length of the tows.

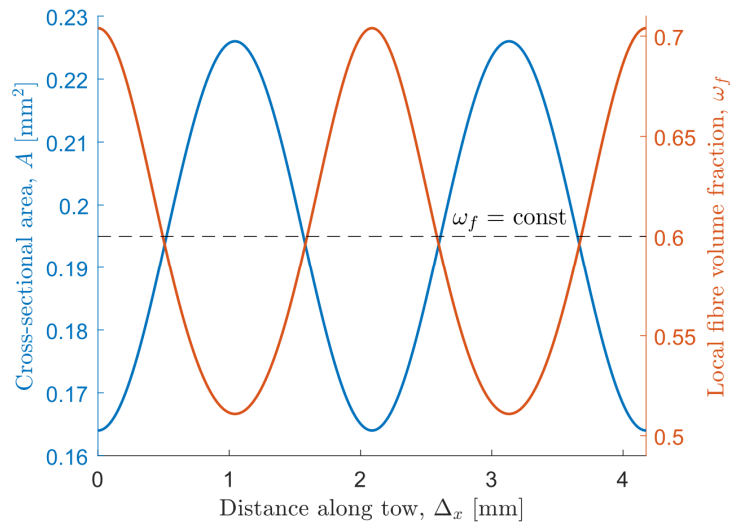


Figure 1. Tow cross-sectional area and intra-tow fibre volume fraction variability along tow length.

Figure 2 provides a bidimensional representation of the RUC considering material variability, with average dimensions represented in Table 3.

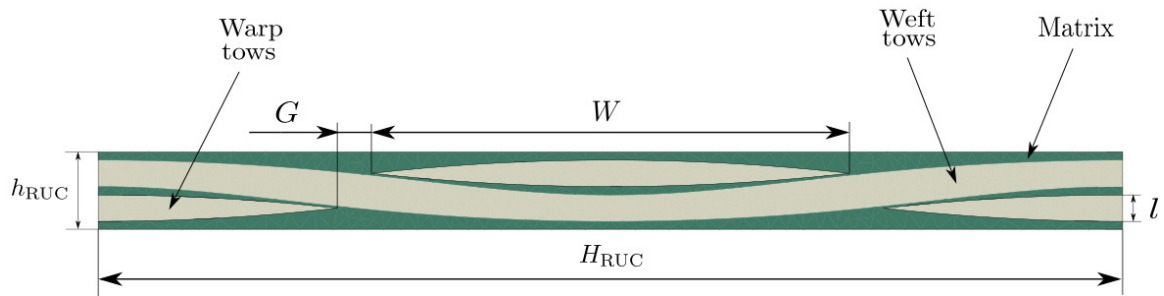


Figure 2. Bi-dimensional representation of the RUC considering cross-sectional area variability.

Table 3. RUCs' average dimensions.

Dimensions	[mm]	Description
H_{RUC}	4.1	RUC width and length
h_{RUC}	0.33	RUC thickness
W	1.9	Tow width
l	0.13	Tow height
G	0.15	Gap between parallel tows

The tow cross-section is assumed to have a special form of the super-ellipse, the power-ellipse, and is defined as:

$$\left|\frac{x}{a}\right| + \left|\frac{y}{b}\right|^{2/n} = 1, \quad (1)$$

with the major and minor ellipse axis, a and b and with the exponent $n = 1.3$.

3. Numerical predictions and discussion

At the microscale, the intention is to homogenise the mechanical properties of the tows through volumetric homogenisation:

$$\sigma_{ij}^0 = \frac{1}{V} \int_V \sigma_{ij} dV = \frac{1}{V} \sum_{k=1}^{N_p} \sigma_{ij}^k V^k, \quad (2)$$

where σ_{ij}^0 represents the homogenised far-field stress tensor, σ_{ij}^k and V^k are the stress component determined at integration point k and associated volume, and N_p is the total number of integration points in the RVE.

After assigning the appropriate constitutive material models for each of the constituents and the fibre-matrix interface, it is possible to address the RVEs' mechanical performance. By generating different RVEs with different fibre volume fractions and by submitting them to different loading conditions, it is possible to generate polynomial curve fitting expressions that enable the evaluation of the mechanical properties for any value of the fibre volume fraction, ω_f .

Considering the fibre volume fraction distribution along the length of the tows represented in Figure 1, and using the polynomial expressions obtained from the micromechanical simulations, the mechanical properties are assigned to each individual element of the mesh of the tows. The tows are modelled by means of C3D8R, three-dimensional, reduced integration hexahedral elements, and the epoxy matrix at the non-homogenised mesoscale, since it represents a complex geometrical part, it is modelled by means of C3D4, three-dimensional tetrahedral continuum solid elements, both with an average size of 0.06 mm.

Numerical predictions are presented in Figure 3, where the homogenised stress-strain curves, obtained with equation (2), are reported for four different loading scenarios: i) uniaxial tension, ii) in-plane shear, iii) biaxial tension and iv) uniaxial tension and in-plane shear. In each curve, different points are indicated and associated with the corresponding contour plot of the matrix damage variable of the intralaminar damage model used to model the tows.

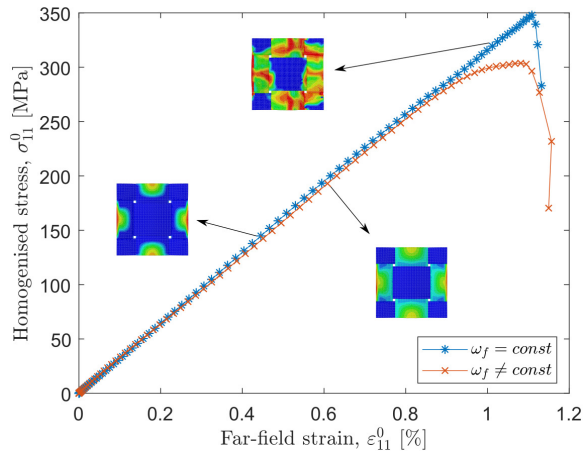


Figure 3.1 Uniaxial tension.

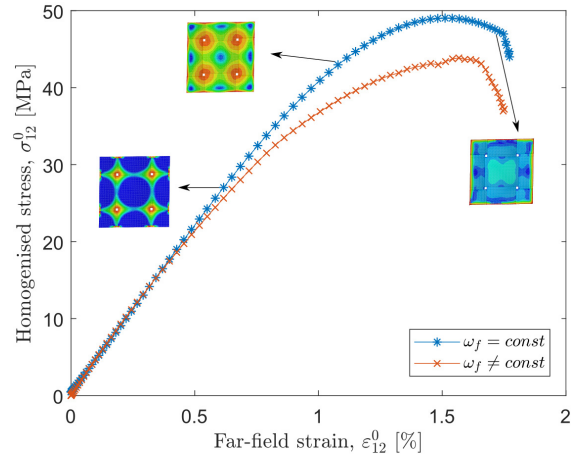


Figure 3.2 In-plane shear.

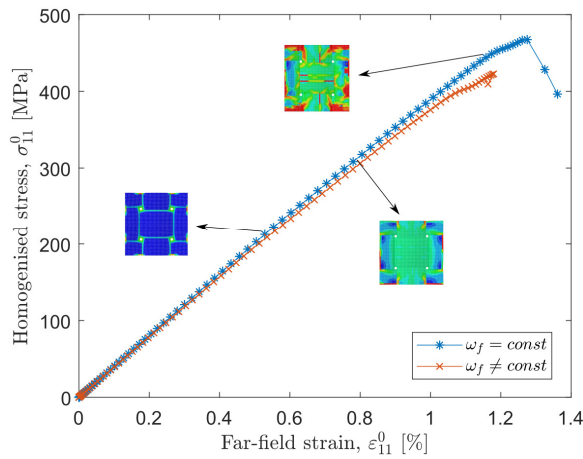


Figure 3.3 Biaxial tension.

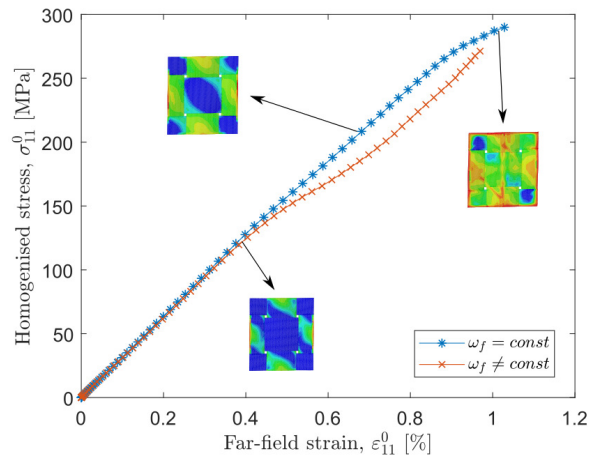


Figure 3.4 Uniaxial tension with in-plane shear.

Figure 3. Numerical predictions of the RUCs' homogenised stress-strain curves for different loading conditions.

Figure 3.1 shows the results for the uniaxial tensile load case. The contour plots presented in the figure validate the present framework, since they fully agree with the observations carried out by Daggumati et al. [24], indicating that in-plane PBCs will concentrate transverse damage at the centre of the crimped weft tows, being associated with a surface layer of the laminate. It can be seen that both RUCs' response coincide until the corresponding final failure of the RUC, which happens earlier for the RUC considering material variability.

Figure 3.2 shows the numerical predictions for the in-plane shear load case. Under a pure shear load, damage tends to localise along the edges of the tows, where there is contact with the embedding matrix, and a difference in shear stiffness between the two materials exist. The most affected region coincides with the one having a higher cross-sectional area, and thus poorer mechanical properties, leading to a higher rate of damage for the RUC considering intra-tow fibre volume fraction variability.

Figure 3.3 shows the results for the biaxial tensile load case. In this case, at the beginning of the simulation, damage tends to concentrate on the edges of the tows, leading later to propagation of damage to the crimp region. It can be seen that the RUC with constant cross-sectional area failed at a higher stress. The RUC with material variability failed catastrophically at a lower applied far-field strain, stopping the simulation.

Figure 3.4 shows the results for the combined in-plane shear with uniaxial tensile load case. A slight combination of the contour plots shown for individual tension (Figure 3.1) and shear (Figure 3.2) is visible. Both simulations stopped before final failure of the RUCs due to excessive element distortion. However, it can be seen that, the RUC with material variability presented a slightly poorer stress-strain response when compared to the RUC with constant cross-sectional area, which may be due to the presence of shear.

4. Conclusions and future work

Using a multiscale approach, the presented work has allowed for the analysis of the mechanical response of a carbon-epoxy plain weave taking into account intra-tow fibre volume fraction variability. In the non-homogenised mesomechanical analyses, the tows are modelled using a transverse isotropic damage model, for which the elastic and strength properties were determined using micromechanical simulations, using different fibre volume fractions. The embedding matrix surrounding the tows is modelled with a coupled elasto-plastic with damage constitutive material model. From the numerical results, it can be seen that material variability of the tows slightly affects the overall response of the material, mainly with the presence of shear, being one of the reasons why the mechanical performance of such materials can be overestimated using computational approaches.

Next steps in this work will involve performing non-homogenised mesomechanical analyses on the RUCs under even more different loading schemes, which will allow the comparison of failure envelopes between RUCs. Tow-matrix decohesion is also a mechanism that is intended to be analysed. It is also desired to perform a comparison between these numerical results and experimental observations.

Acknowledgments

The authors gratefully acknowledge the financial support of the project ICONIC — Improving the crashworthiness of composite transportation structures. ICONIC has received funding from the European Union's Horizon 2020 research and innovation programme under the Marie Skłodowska-Curie grant agreement No 721256. The content reflects only the author's view and the Agency is not responsible for any use that may be made of the information it contains.

References

- [1] M. Bodaghi, A. Vanaerschot, S. V. Lomov, and N. C. Correia, "On the stochastic variations of intra-tow permeability induced by internal geometry variability in a 2/2 twill carbon fabric," *Compos. Part A Appl. Sci. Manuf.*, vol. 101, pp. 444–458, 2017.
- [2] A. Arteiro, G. Catalanotti, A. R. Melro, P. Linde, and P. P. Camanho, "Micro-mechanical analysis of the effect of ply thickness on the transverse compressive strength of polymer composites," *Compos. Part A Appl. Sci. Manuf.*, vol. 79, pp. 127–137, 2015.
- [3] A. Arteiro, G. Catalanotti, A. R. Melro, P. Linde, and P. P. Camanho, "Micro-mechanical analysis of the in situ effect in polymer composite laminates," *Compos. Struct.*, vol. 116, no. 1, pp. 827–840, 2014.
- [4] A. R. Melro, P. P. Camanho, F. M. Andrade Pires, and S. T. Pinho, "Micromechanical analysis of polymer composites reinforced by unidirectional fibres: Part II-Micromechanical analyses," *Int. J. Solids Struct.*, vol. 50, no. 11–12, pp. 1906–1915, 2013.
- [5] G. Soni, R. Singh, M. Mitra, and B. G. Falzon, "Modelling matrix damage and fibre-matrix interfacial decohesion in composite laminates via a multi-fibre multi-layer representative volume element (M2RVE)," *Int. J. Solids Struct.*, vol. 51, no. 2, pp. 449–461, 2014.
- [6] L. F. Varandas, A. Arteiro, M. A. Bessa, A. R. Melro, and G. Catalanotti, "The effect of through-thickness compressive stress on mode II interlaminar crack propagation: A computational micromechanics approach," *Compos. Struct.*, vol. 182, 2017.

- [7] A. R. Melro, P. P. Camanho, F. M. Andrade Pires, and S. T. Pinho, "Micromechanical analysis of polymer composites reinforced by unidirectional fibres: Part I-Constitutive modelling," *Int. J. Solids Struct.*, vol. 50, no. 11–12, pp. 1897–1905, 2013.
- [8] Dassault Systèmes Simulia, "Abaqus 6.14 CAE User Guide," p. 1146, 2014.
- [9] N. W. Tschoegl, "Failure surfaces in principal stress space," *J. Polym. Sci. Part C Polym. Symp.*, vol. 32, no. 1, pp. 239–267, 1971.
- [10] Z. Bazant and B. Oh, "Crack band theory of concrete," *Mater. Struct.*, vol. 16, pp. 155–177, 1983.
- [11] M. L. Benzeggagh and M. Kenane, "Measurement of mixed-mode delamination fracture toughness of unidirectional glass/epoxy composites with mixed-mode bending apparatus," *Compos. Sci. Technol.*, vol. 56, no. 4, pp. 439–449, 1996.
- [12] A. Faggiani and B. G. Falzon, "Predicting low-velocity impact damage on a stiffened composite panel," *Compos. Part A Appl. Sci. Manuf.*, vol. 41, no. 6, pp. 737–749, 2010.
- [13] W. Tan, B. G. Falzon, and M. Price, "Predicting the crushing behaviour of composite material using high-fidelity finite element modelling," *Int. J. Crashworthiness*, vol. 20, no. 1, pp. 60–77, 2015.
- [14] W. Tan, B. G. Falzon, L. N. S. Chiu, and M. Price, "Predicting low velocity impact damage and Compression-After-Impact (CAI) behaviour of composite laminates," *Compos. Part A Appl. Sci. Manuf.*, vol. 71, pp. 212–226, 2015.
- [15] W. Tan and B. G. Falzon, "Modelling the crush behaviour of thermoplastic composites," *Compos. Sci. Technol.*, vol. 134, pp. 57–71, 2016.
- [16] G. Catalanotti, P. P. Camanho, and A. T. Marques, "Three-dimensional failure criteria for fiber-reinforced laminates," *Compos. Struct.*, vol. 95, pp. 63–79, 2013.
- [17] V. Kouznetsova, M. G. D. Geers, and W. A. M. Brekelmans, "Multi-scale constitutive modelling of heterogeneous materials with a gradient-enhanced computational homogenization scheme," *Int. J. Numer. Methods Eng.*, vol. 54, no. 8, pp. 1235–1260, 2002.
- [18] K. Terada, M. Hori, T. Kyoya, and N. Kikuchi, "Simulation of the multi-scale convergence in computational homogenization approaches," *Int. J. Solids Struct.*, vol. 37, no. 16, pp. 2285–2311, 2000.
- [19] S. Ghosh, K. Lee, and S. Moorthy, "Two scale analysis of heterogeneous elastic-plastic materials with asymptotic homogenization and Voronoi cell finite element model," *Comput. Methods Appl. Mech. Eng.*, vol. 132, no. 95, pp. 63–116, 1996.
- [20] A. R. Melro, P. P. Camanho, F. M. Andrade Pires, and S. T. Pinho, "Numerical simulation of the non-linear deformation of 5-harness satin weaves," *Comput. Mater. Sci.*, vol. 61, pp. 116–126, 2012.
- [21] G. Catalanotti, "On the generation of RVE-based models of composites reinforced with long fibres or spherical particles," *Compos. Struct.*, vol. 138, pp. 84–95, 2016.
- [22] P. D. Soden, M. J. Hinton, and A. S. Kaddour, "Lamina properties, lay-up configurations and loading conditions for a range of fibre reinforced composite laminates," *Compos. Sci. Technol.*, vol. 58, pp. 30–51, 2004.
- [23] R. D. B. Sevenois *et al.*, "Avoiding interpenetrations and the importance of nesting in analytic geometry construction for Representative Unit Cells of woven composite laminates," *Compos. Sci. Technol.*, vol. 136, pp. 119–132, 2016.
- [24] S. Daggumati, I. De Baere, W. Van Paepegem, J. Degrieck, J. Xu, and S. V. Lomov, "Local Damage in a 5 – Harness Satin Weave Composite Under Static Tension : Part II - Meso-FE modelling," *Compos. Sci. Technol.*, vol. 71, no. 8, pp. 1–24, 2011.